

Fine-Tuning the Weak-Link Approach: Effect of Ligand Electron Density on the Formation of Rhodium(I) and Iridium(I) Metallomacrocycles

Martin S. Masar III,[†] Maxim V. Ovchinnikov,[†] Chad A. Mirkin,^{*,†} Lev N. Zakharov,^{‡,§} and Arnold L. Rheingold^{‡,§}

Department of Chemistry and Institute for Nanotechnology, 2145 Sheridan Road, Northwestern University, Evanston, Illinois 60208, and Department of Chemistry and Biochemistry, University of Delaware, Newark, Delaware 19716

Received April 14, 2003

A novel bis(phosphinoalkyl–thioether)arene ligand with a fluorinated aryl group (1,4-(Ph₂PCH₂CH₂S)₂C₆F₄) has been synthesized. This ligand has been used to prepare symmetric bimetallic structures with Rh^I and Ir^I metal centers in high yield. Unlike their nonfluorinated counterparts, these complexes can be opened into large macrocyclic structures through straightforward ligand (i.e., carbon monoxide, nitriles, and isocyanides) substitution reactions at the metal–thioether linkage. In addition, the symmetric bimetallic structures have been shown to react with appropriately sized bifunctional aromatic molecules to form three-tiered host–guest structures.

Introduction

There are three general strategies for synthesizing supramolecular multimetallic structures: the directional bonding approach, the symmetry interaction approach, and the weak-link approach.¹ The first two approaches are powerful methods, which rely on thermodynamic control, for assembling a series of ligands and transition metal centers into rigid and often very sophisticated predefined two- and three-dimensional structures. The weak-link approach, introduced by our group, utilizes elements of both thermodynamic and kinetic control² to provide synthetic access to a variety of large open and flexible two- and three-dimensional structures with tailorable size, shape, and charge.³

The weak-link approach targets condensed intermediates that contain strategically placed strong (e.g., metal–phosphine) and weak (e.g., metal–ether, –thioether, –amine,

or –arene) bonds (Scheme 1). The strength of the weak link depends on the transition metal, the heteroatom that forms the weak link with the metal, and the substituents on the aromatic core of the ligand. For example, rhodium–thioether interactions are substantially stronger than their rhodium–ether analogues.^{3d} Consequently, different substitution chemistry must be employed to open each of these structures.

Recently, our group reported a high-yield route for generating neutral dinuclear metallomacrocycles^{3d} and trimetallic prismatic structures^{3g} from flexible hemilabile ligands and simple transition metal precursors via a halide-induced ring-opening method (Scheme 2). In this approach, addition of a halide source to a condensed intermediate under a carbon monoxide atmosphere selectively breaks the metal–weak links to afford neutral macrocycles in nearly quantita-

* To whom correspondence should be addressed. E-mail: camirkin@chem.northwestern.edu.

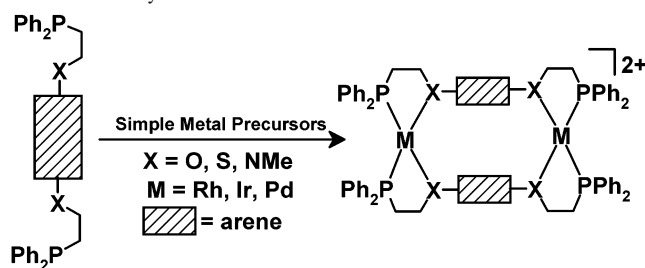
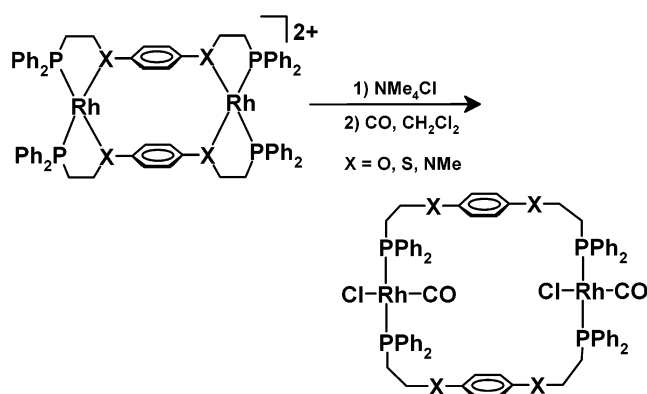
[†] Northwestern University.

[‡] University of Delaware.

[§] Current address: Department of Chemistry and Biochemistry, University of California, San Diego, La Jolla, CA 92093-0358.

- (1) For reviews of these approaches, see: (a) Leininger, S.; Olenyuk, B.; Stang, P. J. *Chem. Rev.* **2000**, *100*, 853. (b) Cotton, F. A.; Lin, C.; Murillo, C. A. *Acc. Chem. Res.* **2001**, *34*, 759. (c) Caulder, D. L.; Raymond, R. N. *Acc. Chem. Res.* **1999**, *32*, 975. (d) Albrecht, M. *Chem. Soc. Rev.* **1998**, *27*, 281. (e) Holliday, B. J.; Mirkin, C. A. *Angew. Chem., Int. Ed.* **2001**, *40*, 2022.
- (2) Holliday, B. J.; Jeon, Y.-M.; Mirkin, C. A.; Stern, C. L.; Incarvito, C. D.; Zakharov, L. N.; Sommer, R. D.; Rheingold, A. L. *Organometallics* **2002**, *21*, 5713.

- (3) (a) Farrell, J. R.; Mirkin, C. A.; Guzei, I. A.; Liable-Sands, L. M.; Rheingold, A. L. *Angew. Chem., Int. Ed. Engl.* **1998**, *37*, 465. (b) Farrell, J. R.; Eisenberg, A. H.; Mirkin, C. A.; Guzei, I. A.; Liable-Sands, L. M.; Incarvito, C. D.; Rheingold, A. L.; L., S. C. *Organometallics* **1999**, *18*, 4858. (c) Holliday, B. J.; Farrell, J. R.; Mirkin, C. A.; Lam, K.-C.; Rheingold, A. L. *J. Am. Chem. Soc.* **1999**, *121*, 6316. (d) Dixon, F. M.; Eisenberg, A. E.; Farrell, J. R.; Mirkin, C. A.; Liable-Sands, L. M.; Rheingold, A. L. *Inorg. Chem.* **2000**, *39*, 3432. (e) Eisenberg, A. H.; Dixon, F. M.; Mirkin, C. A.; Stern, C. L.; Incarvito, C. D.; Rheingold, A. L. *Organometallics* **2001**, *20*, 2052. (f) Liu, X.; Eisenberg, A. H.; Stern, C. L.; Mirkin, C. A. *Inorg. Chem.* **2001**, *40*, 2940. (g) Ovchinnikov, M. V.; Holliday, B. J.; Mirkin, C. A.; Zakharov, L. N.; Rheingold, A. L. *Proc. Nat. Acad. Sci. U.S.A.* **2002**, *99*, 4927. (h) Gianneschi, N. C.; Bertin, P. A.; Nguyen, S. T.; Mirkin, C. A.; Zakharov, L. N.; Rheingold, A. L. *J. Am. Chem. Soc.* **2003**, *125*, 10508.

Scheme 1. Synthetic Outline for Condensed Intermediates^{2,3}Scheme 2. Examples of Halide-Induced Ring Opening^{3d,f}

tive yield.^{3d,f,g} With this approach, 26-membered neutral rings were synthesized from Rh^{I} and Pd^{II} starting materials and a variety of phosphinoaryl–thioether, –ether, and –amine ligands.^{3d,f} In addition, 40-membered trimetallic structures have been synthesized from Rh^{I} and Ir^{I} starting materials and a 3-fold symmetric bis(phosphinoalkyl–thioether)arene ligand.^{3g}

This study examines how one can use electron-withdrawing substituents, such as fluorine atoms, on the aromatic core of the ligand to decrease the strength of the metal–heteroatom bonds⁴ (in this case, $\text{Rh}-\text{S}$ and $\text{Ir}-\text{S}$), which, in turn, affects the type of chemistry that can be used to synthesize the open macrocyclic structures. This not only allows one to bypass the need for the halide-induced method for opening thioether-based structures but also provides a method for preparing cationic macrocycles and more complex host–guest architectures, which were previously inaccessible for thioether-containing macrocycles formed via the weak-link approach.^{3c}

Experimental Section

General Procedures. Unless otherwise noted, all reactions and manipulations were performed under an atmosphere of dry nitrogen using standard Schlenk and glovebox techniques. Tetrahydrofuran (THF) and diethyl ether were distilled over sodium/benzophenone, and CH_2Cl_2 and pentane were distilled over CaH_2 . All solvents were degassed with nitrogen prior to use. Nitromethane- d_3 was purchased from Aldrich. All other deuterated solvents were purchased and used as received from Cambridge Isotopes Laboratories. 2,3,5,6-

Tetrafluorobenzenedithiol⁵ and $[\text{Ir}(\text{COE})_2\text{Cl}]_2$ (COE = cyclooctene)⁶ were prepared according to literature methods. All other chemicals were obtained from commercial sources and used as received unless otherwise noted.

Physical Measurements. $^{31}\text{P}\{^1\text{H}\}$ NMR spectra were recorded on a Varian 300 MHz Gemini FT-NMR spectrometer at 121.53 MHz and referenced relative to an external 85% H_3PO_4 standard. $^{19}\text{F}\{^1\text{H}\}$ NMR spectra were recorded on a Varian 300 MHz Gemini FT-NMR spectrometer at 282.47 MHz and referenced relative to an external CFCl_3 in CDCl_3 standard. ^1H NMR spectra were obtained using a Varian Gemini 300 MHz FT-NMR spectrometer and referenced relative to residual proton resonances in deuterated solvents. $^{13}\text{C}\{^1\text{H}\}$ NMR spectra were obtained using a Varian 300 MHz Gemini FT-NMR spectrometer at 75.5 MHz and referenced relative to residual carbon resonances in deuterated solvents. All chemical shifts are reported in ppm. FT-IR spectra were obtained using a Thermo Nicolet Nexus 670 FT-IR and a solution cell with NaCl windows. Atmospheric pressure chemical ionization (APCI) and electrospray (ES) mass spectra were obtained on a Micromas Quatro II triple quadrupole mass spectrometer. Electron ionization (EI) mass spectra were recorded on a Fisons VG 70-250 SE mass spectrometer. Elemental analyses were obtained from Quantitative Technologies Inc., Whitehouse, NJ.

Synthesis of 1,4-Bis[(2-(diphenylphosphino)ethyl)thio]-2,3,5,6-tetrafluorobenzene (1). In a 100 mL Schlenk flask, 2,3,5,6-tetrafluorobenzenedithiol (1.00 g, 4.67 mmol) and (2-chloroethyl)-diphenylphosphine (2.44 g, 9.81 mmol) were dissolved in acetonitrile (100 mL). Under a flow of nitrogen, cesium carbonate powder (3.29 g, 9.32 mmol) was added to the reaction vessel in one portion. The white suspension was refluxed under nitrogen for 3 h. After being cooled to ambient temperature, the solvent was removed on a rotary evaporator to give a white solid. The solid was washed with water (100 mL) and extracted with methylene chloride (3×175 mL). The combined organic extracts were dried over MgSO_4 , filtered, and evaporated on a rotary evaporator to give a white solid. The solid was recrystallized from $\text{CH}_2\text{Cl}_2/\text{Et}_2\text{O}$ to afford analytically pure **1** (2.56 g, 4.01 mmol, 86%). ^1H NMR (CDCl_3): δ 2.32 (m, SCH_2 , 4H), 2.99 (m, CH_2PPh_2 , 4H), 7.28–7.43 (bm, PPh_2 , 20H). $^{31}\text{P}\{^1\text{H}\}$ NMR (CDCl_3): δ –17.0 (s). $^{19}\text{F}\{^1\text{H}\}$ NMR (CDCl_3): δ –134.51 (s, C_6F_4). $^{13}\text{C}\{^1\text{H}\}$ NMR (CDCl_3): δ 29.2 (d, $J_{\text{C}-\text{P}} = 16$ Hz), 31.5 (d, $J_{\text{C}-\text{P}} = 23$ Hz), 114.4 (m), 128.8 (d, $J_{\text{C}-\text{P}} = 7$ Hz), 129.1 (s), 132.8 (d, $J_{\text{C}-\text{P}} = 19$ Hz), 137.6 (d, $J_{\text{C}-\text{P}} = 14$ Hz), 147.1 (d, $J_{\text{C}-\text{F}} = 249$ Hz). APCI-MS (m/z), $[\text{C}_{34}\text{H}_{28}\text{F}_4\text{P}_2\text{S}_2\text{H}]^+$: calcd = 639.1, expt = 639.1 ($\text{M} + \text{H}^+$). Anal. Calcd for $\text{C}_{34}\text{H}_{28}\text{F}_4\text{P}_2\text{S}_2$: C, 63.94; H, 4.42; P, 9.70; S, 10.04. Found: C, 63.68; H, 4.09; P, 9.63; S, 10.41.

Synthesis of $[(\kappa^2;\mu_2;\kappa^2\text{-}(1,4\text{-bis}[(2\text{-}(\text{diphenylphosphino)ethyl)\text{thio}]\text{-}2,3,5,6\text{-tetrafluorobenzene})_2\text{Rh}_2][\text{BF}_4]_2$ (2). In a glovebox, a mixture of solid $[\text{Rh}(\text{NBD})\text{Cl}]_2$ (NBD = norbornadiene) (50.1 mg, 0.109 mmol) and AgBF_4 (43 mg, 0.220 mmol) was stirred in CH_2Cl_2 (3 mL) for 0.5 h. The resulting reaction mixture was filtered through Celite to remove a light gray precipitate of AgCl . The resulting red-orange solution was diluted with CH_2Cl_2 (10 mL). To this, a solution of **1** (138.4 mg, 0.2167 mmol) in CH_2Cl_2 (15 mL) was added dropwise over 5 min. The solution was stirred for 3 h, over which time it became orange. The solvent was removed in vacuo to give an orange solid. Recrystallization from $\text{CH}_2\text{Cl}_2/\text{Et}_2\text{O}$ afforded an analytically pure orange solid **2** as the sole product as determined by NMR spectroscopy (174 mg, 0.105 mmol, 96%). Orange rectangular single crystals of **2** were grown by diffusion of

(4) For examples of metal–ligand bond weakening caused by electron-withdrawing substituents, see: (a) Edder, C.; Piguat, C.; Bernardinelli, G.; Mareda, J.; Bochet, G. C.; Bunzli, J.-C. G.; Hopfgartner, G. *Inorg. Chem.* **2000**, *39*, 5059. (b) Kadish, K. M.; Wang, L.-L.; Thuriere, A.; Van Caemelbecke, E.; Bear, J. L. *Inorg. Chem.* **2003**, *42*, 834.

(5) Raasch, M. S. *J. Org. Chem.* **1979**, *44*, 2629.

(6) van der Ent, A.; Onderdelinden, A. L. *Inorg. Synth.* **1990**, *28*, 91.

Et₂O into a concentrated CH₂Cl₂ solution of **2**. ¹H NMR (CD₂Cl₂): δ 2.65 (m, SCH₂, 8H), 3.03 (m, CH₂PPh₂, 8H), 7.20–7.43 (bm, PPh₂, 40H). ³¹P{¹H} NMR (CD₂Cl₂): δ 66.0 (d, J_{Rh-P} = 162 Hz). ¹⁹F{¹H} NMR (CD₂Cl₂): δ -128.90 (s, C₆F₄), -153.98 (s, ¹⁰BF₄), -154.04 (s, ¹¹BF₄). ES-MS (*m/z*), [C₆₈H₅₆F₈P₄Rh₂S₄]²⁺: calcd = 741.01; expt = 741.03. Anal. Calcd for C₆₈H₅₆F₁₆P₄Rh₂S₄B₂: C, 49.27; H, 3.41; P, 7.48; S, 7.72. Found: C, 49.25; H, 3.44; P, 7.03; S, 7.79.

Synthesis of [(κ²:μ₂:κ²-(1,4-Bis(2-(diphenylphosphino)ethyl)thio)-2,3,5,6-tetrafluorobenzene)₂Ir₂][BF₄]₂ (3**).** In a glovebox, a mixture of solid [Ir(COE)₂Cl]₂ (50.4 mg, 0.112 mmol) and AgBF₄ (23 mg, 0.118 mmol) was stirred in CH₂Cl₂ (3 mL) for 5 min. Longer reaction times result in decomposition of the Ir starting material as evidenced by a precipitation of a black unidentified material. The resulting reaction mixture was filtered through Celite to remove AgCl. The resulting deep red solution was diluted with CH₂Cl₂ (10 mL). To this, a solution of **1** (72.2 mg, 0.113 mmol) in CH₂Cl₂ (20 mL) was added dropwise over 5 min. The solution was stirred for 3 h. The solvent was removed in vacuo to give an orange solid. Recrystallization from CH₂Cl₂/Et₂O afforded an analytically pure orange solid **3** as the only product as evidenced by NMR spectroscopy (88.2 mg, 0.0481 mmol, 85%). Orange-yellow block single crystals of **3** were grown by diffusion of Et₂O into a dilute CH₂Cl₂/CH₃NO₂ (1:1 v/v) solution of **3**. ¹H NMR (CD₃NO₂): δ 2.50 (m, SCH₂, 8H), 3.07 (m, CH₂PPh₂, 8H), 7.24–7.38 (bm, PPh₂, 40H). ³¹P{¹H} NMR (CD₃NO₂): δ 48.9 (s). ¹⁹F{¹H} NMR (CD₃NO₂): δ -129.4 (s, C₆F₄), -153.81 (s, ¹⁰BF₄), -153.87 (s, ¹¹BF₄). ES-MS (*m/z*): [(C₆₈H₅₆F₈P₄Ir₂S₄)²⁺[BF₄]⁻]⁺, calcd = 1749.1, expt = 1749.3; [C₆₈H₅₆F₈P₄Ir₂S₄]²⁺, calcd = 831.1, expt = 831.2. Anal. Calcd for C₆₈H₅₆F₁₆P₄Ir₂S₄B₂: C, 44.50; H, 3.08; P, 6.75; S, 6.99. Found: C, 45.01; H, 3.10; P, 6.76; S, 7.68.

General Syntheses of [(μ₂-(1,4-Bis(2-(diphenylphosphino)ethyl)thio)-2,3,5,6-tetrafluorobenzene)₂Rh₂(CO)₂(CD₃CN)₂][BF₄]₂ (4**) and [(μ₂-(1,4-Bis(2-(diphenylphosphino)ethyl)thio)-2,3,5,6-tetrafluorobenzene)₂Rh₂(CO)₂(C₆H₅CN)₂][BF₄]₂ (**5**).** CO (2 equiv) was added via a syringe to a 10 mL Schlenk flask containing **2** (10.1 mg, 6:mol) in CD₃NO₂ (3.0 mL) and CD₃CN or C₆H₅CN (0.250 mL). Upon being stirred, the solutions changed color from orange to yellow, indicating the formation of a CO/RCN (R = Ph or CH₃) complex. Upon exposure to a nitrogen atmosphere, complexes **4** and **5** were the sole products as determined by NMR spectroscopy. Upon removal of solvent, complexes **4** and **5** reclosed to form complex **2**. Owing to the lability of the small molecule ligands in **4** and **5**, resolution of the molecular ions in MS and elemental analyses of these complexes were not possible. Data for **4** follow. ¹H NMR (CD₂Cl₂/CD₃CN): δ 1.98 (s, CH₃CN), 2.77 (m, SCH₂, 8H), 3.19 (m, CH₂PPh₂, 8H), 7.25–7.64 (m, PPh₂, 40H). ³¹P{¹H} NMR (CD₂Cl₂/CD₃CN): δ 31.4 (d, J_{Rh-P} = 113 Hz). ¹⁹F{¹H} NMR (CD₂Cl₂/CD₃CN): δ -133.43 (s, C₆F₄), -152.50 (s, ¹⁰BF₄), -152.56 (s, ¹¹BF₄). FT-IR (CD₂Cl₂/CD₃CN): ν_{CO} = 1977 cm⁻¹ (s). ES-MS (*m/z*), [C₆₈H₅₆F₈P₄Rh₂S₄]²⁺: calcd = 741.0; expt = 741.2. Data for **5** follow. ¹H NMR (CD₃NO₂): δ 2.97 (m, SCH₂, 8H), 3.33 (m, CH₂PPh₂, 8H), 7.2–7.9 (br m, PhCN and PPh₂, 50H). ³¹P{¹H} NMR (CD₃NO₂): δ 32.3 (d, J_{Rh-P} = 118 Hz). ¹⁹F{¹H} NMR (CD₃NO₂): δ -132.66 (s, C₆F₄), -152.16 (s, ¹⁰BF₄), -152.21 (s, ¹¹BF₄). FT-IR (CH₂Cl₂): ν_{PhCN} = 2197, ν_{CO} = 1975 cm⁻¹ (s). ES-MS (*m/z*), [C₈₂H₆₆F₈P₄Rh₂S₄N₂]²⁺: calcd = 844.1; expt = 844.0 (M - 2BF₄ - 2(CO)).

Synthesis of [(μ₂-(1,4-Bis(2-(diphenylphosphino)ethyl)thio)-2,3,5,6-tetrafluorobenzene)₂Ir₂(CO)₆][BF₄]₂ (6**).** Compound **3** (7 mg, 4 μmol) was dissolved in CD₂Cl₂ (0.7 mL) in an NMR tube. The orange solution was treated with CO (1 atm) for 30 s. After agitation, the solution changed from orange to pale yellow indicating

formation of **6** as the sole product as determined by NMR spectroscopy. Elemental analysis of **6** was not possible owing to the labile nature of the CO ligands. ¹H NMR (CD₂Cl₂): δ 3.10 (m, SCH₂, 8H), 3.18 (m, CH₂PPh₂, 8H), 7.4–7.8 (m, PPh₂, 40H). ³¹P{¹H} NMR (CD₂Cl₂): δ -9.56 (s). ¹⁹F{¹H} NMR (CD₂Cl₂): δ -133.36 (s, C₆F₄), -152.66 (s, ¹⁰BF₄), -152.80 (s, ¹¹BF₄). FT-IR (CH₂Cl₂): ν_{CO} = 2022 cm⁻¹ (s), 2005 cm⁻¹ (s), 1974 cm⁻¹ (m). ES-MS (*m/z*): [C₇₂H₅₆F₈P₄Ir₂S₄O₄]²⁺, calcd = 887.1, expt = 887.0 (M - 2BF₄ - 2(CO)); [C₇₀H₅₆F₈P₄Ir₂S₄O₂]²⁺, calcd = 859.1, expt = 859.0 (M - 2BF₄ - 4(CO)); [C₆₈H₅₆F₈P₄Ir₂S₄]²⁺, calcd = 831.1, expt = 831.1 (M - 2BF₄ - 6(CO)).

Synthesis of [(μ₂-(1,4-bis(2-(diphenylphosphino)ethyl)thio)-2,3,5,6-tetrafluorobenzene)₂Ir₂(¹³CO)₆][BF₄]₂. The procedure reported above for the synthesis of **6** was repeated with ¹³CO. ³¹P{¹H} NMR (CD₂Cl₂, -20 °C): δ -9.23 (q, J_{C-P} = 12 Hz). ¹⁹F{¹H} NMR (CD₂Cl₂, room temperature): δ -134.3 (s, C₆F₄), -153.5 (s, BF₄). ¹³C{¹H} NMR (CD₂Cl₂, -20 °C): δ 169.74 (t, J_{C-P} = 12 Hz). FT-IR (CH₂Cl₂): ν_{CO} = 1976 cm⁻¹ (s), 1961 cm⁻¹ (s), 1929 cm⁻¹ (m).

General Syntheses of [(μ₂-(1,4-Bis(2-(diphenylphosphino)ethyl)thio)-2,3,5,6-tetrafluorobenzene)₂Rh₂(CNBu^t)₂(CD₃CN)₂][BF₄]₂ (7**) and [(μ₂-(1,4-Bis(2-(diphenylphosphino)ethyl)thio)-2,3,5,6-tetrafluorobenzene)₂Ir₂(CNBu^t)₂(CD₃CN)₂][BF₄]₂ (**8**).** In a glovebox, **2** or **3** (6 μmol) was dissolved in CD₃NO₂ (3.0 mL). Acetonitrile-*d*₃ (250 μL) was added, followed by addition of *tert*-butyl isocyanide (1.4 μL, 12 μmol, 2 equiv). After being stirred for 1 h, compounds **7** or **8** were formed, respectively, as the sole product as determined by ³¹P{¹H} NMR. **7** and **8** were isolated as solids in nearly quantitative yields upon removal of solvent. Data for **7** (11 mg, 5.8 μmol, 96%) follow. ¹H NMR (CD₃NO₂): δ 0.90 (s, CNC(CH₃)₃, 18H), 3.03 (m, SCH₂, 8H), 3.55 (m, CH₂PPh₂, 8H), 7.41–8.00 (bm, PPh₂, 40H). ³¹P{¹H} NMR (CD₃NO₂): δ 24.7 (d, J_{Rh-P} = 124 Hz). ¹⁹F{¹H} NMR (CD₃NO₂): δ -134.26 (s, C₆F₄), -152.29 (s, ¹⁰BF₄), -152.34 (s, ¹¹BF₄). FT-IR (CD₃NO₂; cm⁻¹): ν_{CH₃CN} = 2208 (bs); ν_{BuNC} = 2143 (s). ES-MS (*m/z*): [C₈₂H₈₀F₈P₄Rh₂S₄N₄]²⁺, calcd = 865.4, expt = 865.9 ([M - 2BF₄]²⁺); [C₇₈H₇₄F₈P₄Rh₂S₄N₂]²⁺, calcd = 824.1, expt = 824.3 ([M - 2BF₄ - 2CH₃CN]²⁺); [C₆₈H₅₆F₈P₄Rh₂S₄]²⁺, calcd = 741.0, expt = 741.2 ([M - 2BF₄ - 2MeCN - 2^tBuNC]²⁺). Anal. Calcd for C₈₂H₈₀F₁₆P₄Rh₂S₄N₄B₂: C, 51.67; H, 4.23; N, 2.94; P, 6.51. Found: C, 51.71; H, 4.14; N, 2.92; P, 6.76. Data for **8** (12 mg, 5.8 μmol, 96%) follow. ¹H NMR (CD₃NO₂): δ 0.75 (s, CNC(CH₃)₃, 18H), 3.06 (m, SCH₂, 8H), 3.41 (m, CH₂PPh₂, 8H), 7.42–7.95 (bm, PPh₂, 40H). ³¹P{¹H} NMR (CD₃NO₂): δ 14.3 (s). ¹⁹F{¹H} NMR (CD₃NO₂): δ -134.30 (s, C₆F₄), -152.21 (s, ¹⁰BF₄), -152.27 (s, ¹¹BF₄). FT-IR (CD₃NO₂; cm⁻¹): ν_{CH₃CN} = 2208 (m); ν_{BuNC} = 2136 (s). ESMS (*m/z*): [C₈₂H₈₀F₈P₄Ir₂S₄N₄]²⁺, calcd = 955.2, expt = 955.0 ([M - 2BF₄]²⁺); [C₇₈H₇₄F₈P₄Ir₂S₄N₂]²⁺, calcd = 914.1, expt = 914.0 ([M - 2BF₄ - 2MeCN]²⁺); [C₆₈H₅₆F₈P₄Ir₂S₄]²⁺, calcd = 831.1, expt = 831.2 ([M - 2BF₄ - 2MeCN - 2^tBuNC]²⁺). Anal. Calcd for C₈₂H₈₀F₁₆P₄Ir₂S₄N₄B₂: C, 47.21; H, 3.87; N, 2.69; P, 5.94. Found: C, 47.23; H, 3.90; N, 2.68; P, 5.86.

General Syntheses of [(μ₂-(1,4-Bis(2-(diphenylphosphino)ethyl)thio)-2,3,5,6-tetrafluorobenzene)₂Rh₂(μ₂-2,3,5,6-tetramethyl-1,4-phenylene diisocyanide)(CD₃CN)₂][BF₄]₂ (9**), [(μ₂-(1,4-Bis(2-(diphenylphosphino)ethyl)thio)-2,3,5,6-tetrafluorobenzene)₂Ir₂(μ₂-2,3,5,6-tetramethyl-1,4-phenylene diisocyanide)(CD₃CN)₂][BF₄]₂ (**10**), [(μ₂-(1,4-Bis(2-(diphenylphosphino)ethyl)thio)-2,3,5,6-tetrafluorobenzene)₂Rh₂(μ₂-2,3,5,6-tetramethyl-1,4-phenylene diisocyanide)(CD₃CN)₂][BF₄]₂ (**11**), and [(μ₂-(1,4-Bis(2-(diphenylphosphino)ethyl)thio)-2,3,5,6-tetrafluorobenzene)₂Ir₂(μ₂-1,4-phenylene diisocyanide)(CD₃CN)₂][BF₄]₂ (**12**).** The synthetic methodology used to isolate the trilayered complexes **9**–**12** was

identical with that for complexes **7** and **8**, except 1 equiv of 2,3,5,6-tetramethyl-1,4-phenylene diisocyanide (DDI = durenyl diisocyanide) or 1,4-phenylene diisocyanide (PDI) were used in place of *tert*-butyl isocyanide and reacted with **2** or **3** (15 μmol). Longer reaction times (>5 h) were required for the formation of the PDI structures (**11**, **12**). The lability of the CH_3CN ligand precludes complete drying of these complexes. Therefore, some CH_3CN was found in some of the elemental analyses of these complexes. Data for **9** (27 mg, 14 μmol , 94%) follow. ^1H NMR (CD_3NO_2): δ 1.39 (s, durene $-\text{CH}_3$, 12H), 3.14 (m, SCH_2 , 8H), 3.24 (m, CH_2PPh_2 , 8H), 7.27–8.00 (bm, PPh_2 , 40H). $^{31}\text{P}\{^1\text{H}\}$ NMR (CD_3NO_2): δ 23.0 (d, $J_{\text{Rh-P}} = 122$ Hz). $^{19}\text{F}\{^1\text{H}\}$ NMR (CD_3NO_2): δ -135.68 (s, C_6F_4), -152.15 (s, $^{10}\text{BF}_4$), -152.19 (s, $^{11}\text{BF}_4$). FT-IR (CD_3NO_2 ; cm^{-1}): $\nu_{\text{CH}_3\text{CN}} = 2208$ (s); $\nu_{\text{DDI}} = 2095$ (s). ES-MS (m/z): $[\text{C}_{84}\text{H}_{74}\text{F}_8\text{P}_4\text{Rh}_2\text{S}_4\text{N}_4]^{2+}$, calcd = 874.6, expt = 874.8 ($[\text{M} - 2\text{BF}_4]^{2+}$). Anal. Calcd for $\text{C}_{84}\text{H}_{74}\text{F}_{16}\text{P}_4\text{Rh}_2\text{S}_4\text{N}_4\text{B}_2\text{CH}_3\text{CN}$: C, 52.59; H, 3.95; N, 3.57; P, 6.31. Found: C, 53.09; H, 4.25; N, 4.68; P, 5.99. Data for **10** (29 mg, 14 μmol , 92%) follow. ^1H NMR (CD_3NO_2): δ 1.37 (s, durene CH_3 , 18H), 3.14 (bm, $\text{SCH}_2\text{CH}_2\text{PPh}_2$, 16H), 7.09–8.02 (bm, PPh_2 , 40H). $^{31}\text{P}\{^1\text{H}\}$ NMR (CD_3NO_2): δ 13.8 (s). $^{19}\text{F}\{^1\text{H}\}$ NMR (CD_3NO_2): δ -135.64 (s, C_6F_4), -152.16 (s, $^{10}\text{BF}_4$), -152.21 (s, $^{11}\text{BF}_4$). FT-IR (CD_3NO_2): $\nu_{\text{CH}_3\text{CN}} = 2175$ (s); $\nu_{\text{DDI}} = 2085$ (s). ES-MS (m/z): $[\text{C}_{84}\text{H}_{74}\text{F}_8\text{P}_4\text{Ir}_2\text{S}_4\text{N}_4]^{2+}$, calcd = 964.2, expt = 964.4 ($[\text{M} - 2\text{BF}_4]^{2+}$). Anal. Calcd for $\text{C}_{84}\text{H}_{74}\text{F}_{16}\text{P}_4\text{Ir}_2\text{S}_4\text{N}_4\text{B}_2\cdot 2\text{CH}_3\text{CN}$: C, 48.42; H, 3.69; N, 3.87; P, 5.67. Found: C, 48.50; H, 3.74; N, 3.97; P, 5.57. Data for **11** (25 mg, 13 μmol , 89%) follow. ^1H NMR (CD_3NO_2): δ 3.07 (m, SCH_2 , 8H), 3.31 (m, CH_2PPh_2 , 8H), 7.23–7.92 (bm, PPh_2 and PDI, 44H). $^{31}\text{P}\{^1\text{H}\}$ NMR (CD_3NO_2): δ 25.5 (d, $J_{\text{Rh-P}} = 121$ Hz). $^{19}\text{F}\{^1\text{H}\}$ NMR (CD_3NO_2): δ -135.22 (s, C_6F_4), -151.63 (s, $^{10}\text{BF}_4$), -151.69 (s, $^{11}\text{BF}_4$). FT-IR (CD_3NO_2): $\nu_{\text{CH}_3\text{CN}} = 2204$ (s); $\nu_{\text{PDI}} = 2100$ (s). ES-MS (m/z): $[\text{C}_{80}\text{H}_{66}\text{F}_8\text{P}_4\text{Rh}_2\text{S}_4\text{N}_4]^{2+}$, calcd = 846.1, expt = 845.6 ($[\text{M} - 2\text{BF}_4]^{2+}$). Anal. Calcd for $\text{C}_{80}\text{H}_{66}\text{F}_{16}\text{P}_4\text{Rh}_2\text{S}_4\text{N}_4\text{B}_2\cdot\text{CH}_3\text{NO}_2$: C, 50.42; H, 3.61; N, 3.64; P, 6.43. Found: C, 50.44; H, 3.61; N, 3.84; P, 6.03. Data for **12** follow. ^1H NMR (CD_3NO_2): δ 3.12 (m, SCH_2 , 8H), 3.34 (m, CH_2PPh_2 , 8H), 7.22–8.05 (m, PPh_2 and PDI, 44H). $^{31}\text{P}\{^1\text{H}\}$ NMR (CD_3NO_2): δ 14.2 (s). $^{19}\text{F}\{^1\text{H}\}$ NMR (CD_3NO_2): δ -133.94 (s, C_6F_4), -152.23 (s, $^{10}\text{BF}_4$), -152.35 (s, $^{11}\text{BF}_4$). FT-IR (CD_3NO_2): $\nu_{\text{CH}_3\text{CN}} = 2174$ (s); $\nu_{\text{PDI}} = 2094$ (s). ES-MS (m/z): $[\text{C}_{80}\text{H}_{66}\text{F}_8\text{P}_4\text{Ir}_2\text{S}_4\text{N}_4]^{2+}$, calcd = 936.1, expt = 936.3 ($[\text{M} - 2\text{BF}_4]^{2+}$). Anal. Calcd for $\text{C}_{80}\text{H}_{66}\text{F}_{16}\text{P}_4\text{Ir}_2\text{S}_4\text{N}_4\text{B}_2\cdot 2\text{CH}_3\text{CN}$: C, 47.36; H, 3.41; N, 3.94; P, 5.82. Found: C, 47.96; H, 3.67; N, 4.35; P, 5.27.

General Syntheses of $(\mu^2\text{-}(1,4\text{-Bis}(2\text{-}(\text{diphenylphosphino})\text{ethyl})\text{thio})\text{-}2,3,5,6\text{-tetrafluorobenzene})_2\text{Rh}_2(\text{CO})_4\text{I}_2$ (13**) and $(\mu^2\text{-}(1,4\text{-Bis}(2\text{-}(\text{diphenylphosphino})\text{ethyl})\text{thio})\text{-}2,3,5,6\text{-tetrafluorobenzene})_2\text{Ir}_2(\text{CO})_4\text{I}_2$ (**14**).** An excess of 2 molar equiv of $[\text{Me}_4\text{N}]\text{I}$ (3 mg, 0.03 mmol) was added to a flask containing **2** or **3** (0.0061 mmol). To this, CO-saturated nitromethane- d_3 (3.0 mL) was added under a pressure of CO to give a yellow solution and a white precipitate ($[\text{Me}_4\text{N}][\text{BF}_4]$). After filtering of the mixture through Celite, the yellow solution contained only **13** or **14**, as determined by NMR spectroscopy. Removal of solvent yielded analytically pure compounds **13** and **14**. The lability of the CO ligands precluded elemental combustion analysis for these complexes. Data for **13** (11 mg, 5.9 μmol , 98%) follow. ^1H NMR (CD_2Cl_2): δ 3.13 (m, SCH_2 , 8H), 3.28 (s, CH_2PPh_2 , 8H), 7.30–7.80 (m, PPh_2 , 40H). $^{31}\text{P}\{^1\text{H}\}$ NMR (CD_2Cl_2): δ 21.3 (d, $J_{\text{Rh-P}} = 122$ Hz). $^{19}\text{F}\{^1\text{H}\}$ NMR (CD_3NO_2): δ -133.77 (s, C_6F_4). FT-IR (CD_3NO_2): $\nu_{\text{CO}} = 1971$ cm^{-1} (s), 2005 cm^{-1} (w). ES-MS (m/z): $[\text{C}_{68}\text{H}_{56}\text{F}_8\text{P}_4\text{Rh}_2\text{S}_4\text{ICO}]^+$, calcd = 1636.9, expt = 1637.1 ($[\text{M} - \text{I} - 3\text{CO}]^+$). Data for **14** (12 mg, 5.9 μmol , 97%) follow. ^1H NMR (CD_3NO_2): δ 3.13 (bs, SCH_2 , 8H), 3.52 (bm, CH_2PPh_2 , 8H), 7.12–

Table 1. Crystallographic Data and Data Collection, and Refinement Parameters for **2** and **3**

	2·2C ₆ H ₆	3·2CH ₂ Cl ₂
formula	C ₈₀ H ₆₈ B ₂ F ₁₆ P ₄ Rh ₂ S ₄	C ₇₀ H ₆₀ B ₂ Cl ₄ F ₁₆ Ir ₂ P ₄ S ₄
fw	1812.90	2005.12
cryst syst	monoclinic	monoclinic
space group	<i>P</i> 2 ₁ / <i>c</i>	<i>P</i> 2 ₁ / <i>c</i>
<i>a</i> (Å)	16.185(2)	16.243(2)
<i>b</i> (Å)	13.778(2)	13.723(2)
<i>c</i> (Å)	17.615(2)	17.778(2)
β (deg)	112.513(3)	112.203(2)
<i>V</i> (Å ³)	3834.6(8)	3669.1(9)
<i>Z</i> , <i>Z'</i>	2, 0.5	2, 0.5
$2\theta_{\text{max}}$ (deg)	56.6	56.6
temp, K	218(2)	120(6)
X-radiation (λ , Å)	Mo K α (0.710 73)	Mo K α (0.710 73)
indpdt reflns	6998 [<i>R</i> _{int} = 0.0228]	8474 [<i>R</i> _{int} = 0.0385]
<i>R</i> ₁ , ^a <i>wR</i> ₂ ^b	0.0384, 0.1002	0.0468, 0.1170
largest diff peak and hole (e ⁻ Å ⁻³)	1.256, -0.757	2.846, -1.018
GOF	1.038	1.044

$$^a R = \sum ||F_o| - |F_c|| / \sum |F_o|. \quad ^b R(wF^2) = \{ \sum [w(F_o^2 - F_c^2)^2] / \sum [w(F_o^2)^2] \}^{1/2}; \\ w = 1 / [\sigma^2(F_o^2) + (aP)^2 + bP], \quad P = [2F_c^2 + \max(F_o, 0)] / 3.$$

7.95 (m, PPh_2 , 40H). $^{31}\text{P}\{^1\text{H}\}$ NMR (CD_3NO_2): δ 19.8 (s). $^{19}\text{F}\{^1\text{H}\}$ NMR (CD_3NO_2): δ -135.1 (s, C_6F_4). FT-IR (CD_3NO_2): $\nu_{\text{CO}} = 1973$ cm^{-1} (s), 2015 cm^{-1} (w). APCI-MS (m/z): $[\text{C}_{72}\text{H}_{56}\text{F}_8\text{P}_4\text{Ir}_2\text{S}_4\text{I}_2\text{O}_4\text{H}]^+$, calcd = 2028.9, expt = 2028.5 ($[\text{M} + \text{H}]^+$).

X-ray Crystal Structure Determination of **2 and **3**.** Diffraction intensity data were collected with Bruker Smart Apex CCD diffractometers. Crystal data, data collection, and refinement parameters are given in Table 1. The structures were solved using direct methods, completed by subsequent difference Fourier syntheses, and refined by full matrix least-squares procedures on F^2 . SADABS absorption corrections were applied, $T_{\text{min}}/T_{\text{max}} = 0.79$ (**2**) and 0.62 (**3**). (Sheldrick, G. M. *SADABS (2.01)*, Bruker/Siemens Area Detector Absorption Correction Program; Bruker AXS: Madison, WI, 1998). Non-hydrogen atoms were refined with anisotropic displacement coefficients, and the hydrogen atoms were refined in a riding model with isotropic parameters equal to 1.2 times the equivalent U_{iso} of the bonded non-H atoms. In the structures of **2**, the BF_4 anion is disordered over three positions with occupation multiplicity $\mu = 0.333$. All software and sources scattering factors are contained in the SHELXTL (5.10) program package (G. Sheldrick, Bruker XRD, Madison, WI). Crystallographic data (excluding structure factors) for the structures reported in this paper have been deposited with the Cambridge Crystallographic Data Centre as supplementary publication nos. CCDC-20570 (**2**) and CCDC-207571 (**3**).

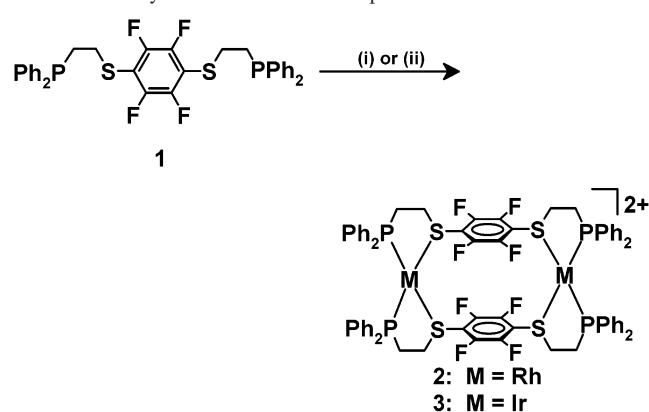
Results

Ligand Synthesis. Ligand **1** was prepared by alkylation of 2,3,5,6-tetrafluorobenzenedithiol⁵ with (2-chloroethyl)-diphenylphosphine in acetonitrile in the presence of cesium carbonate (see Experimental Section). The ligand is a mildly air-sensitive white solid and has been characterized by ^1H , $^{19}\text{F}\{^1\text{H}\}$, $^{31}\text{P}\{^1\text{H}\}$, and $^{13}\text{C}\{^1\text{H}\}$ NMR spectroscopies, mass spectrometry, and elemental analysis. The $^{31}\text{P}\{^1\text{H}\}$ NMR chemical shift of **1** (δ : -17.0 ppm) compares well with its benzene-^{3d} and triphenylbenzene-based^{3g} analogues (δ : -15.7 ppm and -16 ppm, respectively). All other data are consistent with the formulated structure.

Condensed Macrocycles, **2 and **3**.** The condensed intermediates **2** and **3** were synthesized via methodologies

Formation of Rh^I and Ir^I Metallomacrocycles

Scheme 3. Synthetic Outline for Complexes **2** and **3**^a



^a All reactions were performed at 25 °C. All counterions are BF₄⁻. Reagents and yields: (i) [Rh(NBD)][BF₄], CH₂Cl₂, 96%; (ii) [Ir(COE)₂][BF₄], CH₂Cl₂, 85%.

analogous to published procedures (Scheme 3).^{3d,g} Ligand **1**, dissolved in CH₂Cl₂, was reacted with [Rh(NBD)][BF₄] or [Ir(COE)₂][BF₄] (generated in situ via silver(I) abstraction) in CH₂Cl₂ to generate complexes **2** and **3**, respectively. In these reactions, the weakly coordinating alkene ligands of the metal precursors are displaced by the phosphine and thioether moieties of the ligand to produce the condensed intermediates in high yield. Compounds **2** and **3** have been fully characterized in solution (see Experimental Section) as well as in the solid state via single-crystal X-ray diffraction studies (vide infra).

The ³¹P{¹H} NMR spectra of **2** and **3** compare well with literature values for isostructural Rh^I and Ir^I complexes. Rhodium-containing compound **2** exhibits a characteristic doublet at δ 66.0 ppm (*J*_{Rh-P} = 162 Hz) which is diagnostic of a *cis*-phosphine, *cis*-thioether structure. For example, the benzene-based analogue of this complex shows a doublet at δ 64 ppm (*J*_{Rh-P} = 161 Hz).^{3d} Iridium-containing compound **3** exhibits a singlet at 48.9 ppm which compares well with reported *cis*-phosphine, *cis*-thioether mono- and trimetallic Ir^I complexes with phosphinoalkyl-thioether ligands in similar coordination environments (47.3 and 49 ppm, respectively).^{3g,7}

Solid-State Characterization of 2 and 3. Yellow single crystals of **2** were grown by diffusion of benzene into a concentrated CH₂Cl₂ solution of **2**. Orange-yellow block single crystals of **3** were grown by diffusion of Et₂O into a dilute CH₂Cl₂/CH₃NO₂ (1:1 v/v) solution of **3**. The structures of **2** and **3**, which are nearly superimposable, were determined by single-crystal X-ray diffraction methods and are consistent with their proposed solution structures (Figure 1). Selected bond distances and angles are shown in Table 2. The two fluorinated aryl moieties in **2** and **3** are parallel planar and separated by 3.42 and 3.35 Å, respectively, which compares well with other condensed intermediates that contain π-π stacking interactions.^{3a,3,3,8} The metal-metal distance in both complexes (8.60 Å in **2**, 8.67 Å in **3**) are longer than those in the analogous Rh^I *cis*-phosphine, *cis*-

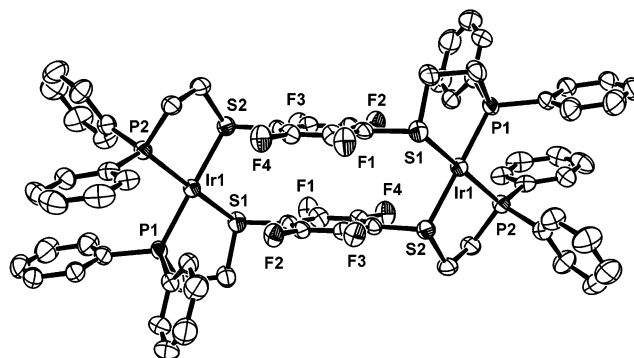


Figure 1. Thermal ellipsoid drawing of **3** showing the labeling scheme for selected atoms and ellipsoids at 30% probability. Hydrogen atoms, counterions, and CH₂Cl₂ solvent are omitted for clarity.

Table 2. Selected Structural Data for [1,4-(Ph₂PCH₂CH₂S)₂C₆F₄]₂M₂[BF₄]₂ (M = Rh (**2**), Ir (**3**))

	2 ·2C ₆ H ₆	3 ·2CH ₂ Cl ₂
M-M (Å)	8.603(1)	8.667(1)
M-S(1) (Å)	2.3169(9)	2.335(2)
M-S(2) (Å)	2.3545(7)	2.316(2)
M-P(1) (Å)	2.2431(7)	2.255(2)
M-P(2) (Å)	2.242(1)	2.247(2)
C ₆ F ₄ (centroid)-C ₆ F ₄ (centroid) (Å)	3.415	3.346
S(1)-M-S(2) (deg)	93.24(3)	93.27(6)
P(1)-M-S(1) (deg)	84.60(3)	84.89(6)
P(1)-M-P(2) (deg)	96.84(3)	97.29(6)
P(2)-M-S(2) (deg)	84.99(3)	84.39(6)

thioether complex with a benzene-based backbone (8.38 Å).^{3d} Each metal center exhibits slightly distorted square planar geometry with two *cis*-phosphine and two *cis*-thioether moieties; the P-M-P, S-M-S, and P-M-S angles range from 84.39(6) to 97.29(6)°. The metal-sulfur distances for each of these complexes are in the 2.316(2)–2.3545(7) Å range, and the metal-phosphine bonds are in the 2.242(2)–2.255(2) Å range. The metal-heteroatom bonds in **2** and **3** are very similar in length to their Rh^I benzene-based analogue (average Rh-S, 2.25 Å; average Rh-P, 2.35 Å).^{3d}

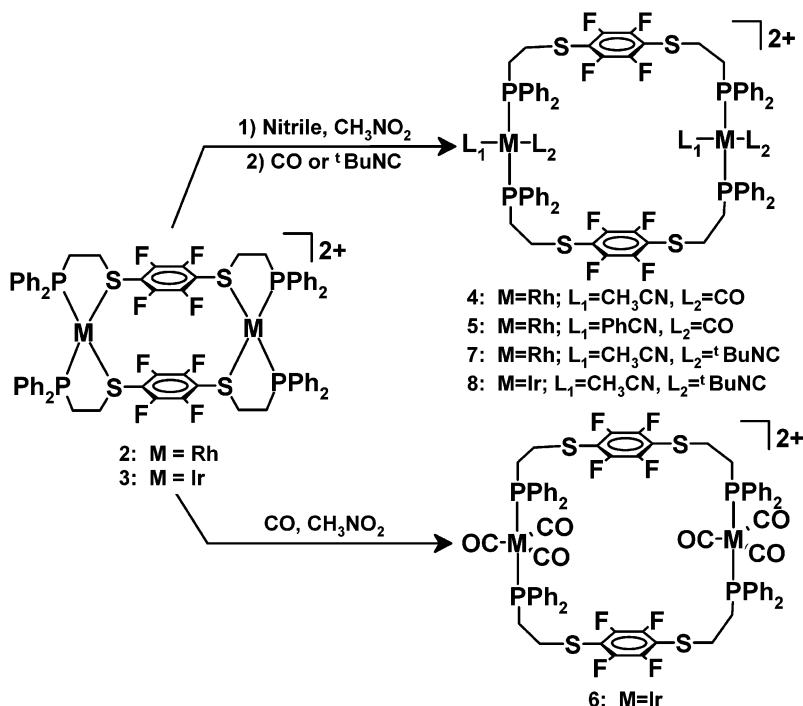
Cationic Macrocycles, 4–8. Treatment of CD₃NO₂ solutions of **2** with 2 equiv of acetonitrile or benzonitrile followed by exposure to CO leads to displacement of the relatively weak metal-thioether bonds to quantitatively yield open 26-membered macrocyclic ring structures **4** and **5** (Scheme 4). Compounds **4** and **5** have been characterized by mass spectrometry, as well as ¹H, ¹⁹F{¹H}, and ³¹P{¹H} NMR and FT-IR spectroscopies. Compounds **4** and **5** exhibit ³¹P{¹H} NMR chemical shifts (δ 31.4 and 32.3 ppm, respectively) and coupling constants (*J*_{Rh-P} = 113 and 118 Hz, respectively) that compare well with mononuclear *trans*-phosphine, *trans*-CO/MeCN rhodium complexes (29.4 ppm, 119 Hz).^{8,9} The FT-IR spectra of each of these complexes show a single CO band in the 1975–1977 cm⁻¹ range which supports the structural assignment formulated in Scheme 4.

To form the cationic iridium complex **6**, a CD₂Cl₂ solution of condensed intermediate **3** was reacted with CO (1 atm) to yield a pale yellow solution containing the hexacarbonyl

(7) Sanger, A. R. *Can. J. Chem.* **1983**, *61*, 2214.

(8) Shriver, D. F.; Atkins, P.; Langford, C. H. *Inorganic Chemistry*, 2nd ed.; W. H. Freeman: New York, 1997.

(9) Siedle, A. R.; Gleason, W. B.; Newmark, R. A.; Skarjune, R. P.; Lyon, P. A.; Markell, C. G.; Hodgson, K. O.; Roe, A. L. *Inorg. Chem.* **1990**, *29*, 1667.

Scheme 4. Synthetic Outline for Cationic Complexes 4–8^a

^a All reactions were performed at 25 °C. All counterions are BF₄⁻.

adduct which is unaffected by the removal of the CO atmosphere with nitrogen (Scheme 4). However, upon prolonged exposure to vacuum (>2 h), the CO ligands can be completely removed to yield condensed intermediate **3**. Compound **6** has been characterized by ¹H, ¹³C{¹H}, ¹⁹F{¹H}, and ³¹P{¹H} NMR and FT-IR spectroscopies, as well as mass spectrometry. On the basis of the NMR and IR spectra of **6**, the binuclear macrocycle contains trigonal bipyramidal metal centers with two axial phosphine moieties and three equatorial CO ligands. Complex **6** exhibits a ³¹P{¹H} NMR chemical shift (−9.56 ppm) that is similar to that for a related mononuclear complex ([Ir(PPh₃)₂(CO)₃]BF₄; −1.19 ppm).¹⁰ The presence of three bands (2022 s, 2005 s, 1974 m) in the infrared spectrum suggests a distortion in the local *D*_{3h} symmetry of each metal center as is expected for this complex. The asymmetry of the ligand induces the splitting of the E' mode expected for a *D*_{3h} symmetry group and a weak activity for the infrared-inactive A'₁ vibration.¹¹ As further evidence for the hexacarbonyl adduct, a low-temperature NMR study was conducted with ¹³C-labeled carbon monoxide. Consistent with the structural assignment of **6**, at −20 °C, the ³¹P{¹H} NMR spectrum of ¹³CO-labeled **6** exhibits a quartet at δ −9.56 (*J*_{P-C} = 12 Hz) and the ¹³C{¹H} NMR spectrum shows a triplet at δ 169.7 (*J*_{C-P} = 12 Hz). In addition, the FT-IR spectrum of ¹³CO-labeled **6** shows three bands at 1976 (s), 1961 (s), and 1929 (m) cm⁻¹. Attempts to synthesize nitrile/carbon monoxide complexes (analogous to **4** and **5**) with Ir^I metal centers under an atmosphere of CO were unsuccessful. It is known that

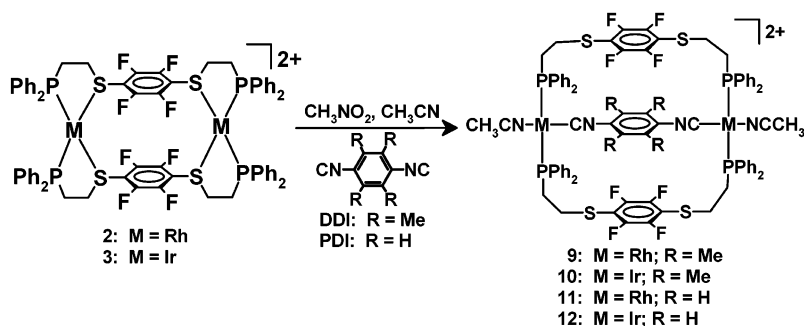
nitriles coordinated to iridium(I) bis(phosphine) complexes are often readily replaced by CO under mild conditions.¹²

The steric environment around the metal centers of these macrocycles can be controlled easily by changing the size of the small molecules used as the substituting ligands. In lieu of carbon monoxide, isoelectronic isocyanides (in the presence of acetonitrile) can be used to break the metal–thioether bond. For example, compounds **2** and **3** can be treated with a 100-fold excess of acetonitrile followed by addition of 2 equiv of *tert*-butyl isocyanide in deuterated nitromethane to yield complexes **7** and **8**, respectively (Scheme 4). Compounds **7** and **8** have been characterized by ¹H, ¹⁹F{¹H}, and ³¹P{¹H} NMR and FT-IR spectroscopy, as well as mass spectrometry and elemental analyses. On the basis of ³¹P{¹H} NMR and FT-IR, the metal centers are each bound to two *trans*-phosphine and *trans*-MeCN/isocyanide ligands in a square planar arrangement. The ³¹P{¹H} NMR spectrum of **7** (δ 24.7 ppm, d, *J*_{Rh-P} = 124 Hz) compares well with an isostructural bis(phosphinoalkyl ether)anthracene complex (δ 20.3, d, *J*_{Rh-P} = 122 Hz).^{3c} Consistent with its assigned structure, the FT-IR spectrum of **7** shows single bands for the bound small molecules (ν_{CH₃CN} = 2208; ν_{BuNC} = 2143 cm⁻¹). The ³¹P{¹H} NMR spectrum of **8** has a single resonance at 14.3 ppm, which is similar to other open square planar Ir^I bis(phosphine) macrocycles.^{3g} The FT-IR spectrum of **8** (ν_{CH₃CN} = 2208; ν_{BuNC} = 2136 cm⁻¹) is similar to that of **7**. These data along with the ES-MS and elemental analysis support the formulation of **8** as shown in Scheme 4.

(10) Mirkin, C. A. Unpublished results.

(11) Adams, D. M. *Metal–Ligand and Related Vibrations*; Edward Arnold Ltd.: London, 1967; p 105.

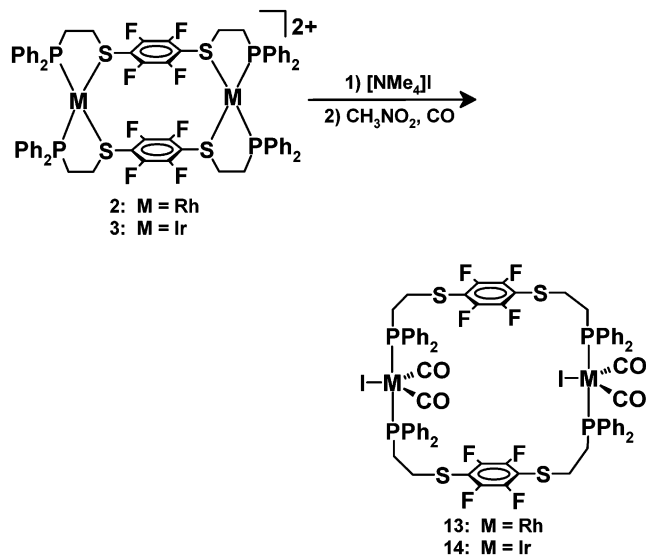
(12) (a) Chin, C. S.; Lee, B.; Kim, S. *Organometallics* **1993**, *12*, 1462. (b) Basato, M.; Longato, B.; Morandini, F.; Bresadola, S. *Inorg. Chem.* **1984**, *23*, 3972. (c) Burrell, A. K.; Roper, W. R. *Organometallics* **1990**, *9*, 1905.

Scheme 5. Synthetic Outline for Cationic Metal-Mediated Host–Guest Complexes **9–12**^a


^a All reactions were performed at 25 °C. All counterions are BF₄⁻.

Metal-Mediated Host–Guest Complexes, 9–12. The three-tiered structures **9–12** were synthesized in a manner similar to that for the *tert*-butyl isocyanide/acetonitrile complexes above. Instead of 2 equiv of the monodentate isocyanide, 1 equiv of a bifunctional diisocyanide (2,3,5,6-tetramethyl-1,4-phenylene diisocyanide (DDI) or 1,4-phenylene diisocyanide (PDI)) was used to span the metal centers intramolecularly (Scheme 5). Compounds **9–12** have been characterized by ¹H, ¹⁹F{¹H}, and ³¹P{¹H} NMR and FT-IR spectroscopy, as well as mass spectrometry and elemental analysis. Compounds **9** and **11** exhibit comparable chemical shifts (δ 23.0 and 25.5 ppm, respectively) and coupling constants ($J_{\text{Rh-P}} = 122$ and 121 Hz, respectively) in their ³¹P{¹H} NMR spectra to their analogous ether-based rhodium(I) metal-bound host–guest complexes (δ 19.8 ppm, $J_{\text{Rh-P}} = 122$ Hz).^{3c} Iridium(I)-containing complexes **10** and **12** have ³¹P{¹H} NMR spectra similar to those of the nitrile/isonitrile complex **8**. The ν_{MeCN} bands and $\nu_{\text{isonitrile}}$ bands of **9–12** show shifts to lower wavenumbers in their FT-IR spectra as compared to free MeCN and the free isonitriles from which they are derived due to complexation to the cationic metal centers. It has been shown that the bands in the FT-IR spectra of η^1 -N-bound nitriles shift to larger wavenumbers upon complexation.¹³ This phenomenon is due to the coupling of the CN vibration with that of the dative N → M bond and the slight strengthening of the CN bond as the weakly antibonding character of the nitrogen lone pair orbital decreases when it becomes the N → M bonding orbital. However, the soft Lewis acid (Rh^I and Ir^I) centers are capable of π -back-bonding to the nitrile to a sufficient extent to offset the frequency-increasing factors.¹³

Neutral Macrocycles 13 and 14. The neutral iodo-carbonyl complexes **13** and **14** were synthesized by adding an excess of [Me₄N]I to intermediate **2** or **3**, respectively, followed by dissolution in CO-saturated deuterated nitromethane and filtering of the mixture to remove excess [Me₄N]I and [Me₄N]BF₄ formed during the reaction (Scheme 6). The resulting solutions contained one product as evidenced by the ³¹P{¹H} NMR spectra. Compounds **13** and **14** were characterized by ¹H, ¹⁹F{¹H}, and ³¹P{¹H} NMR and FT-IR spectroscopies, as well as mass spectrometry. The ³¹P{¹H} NMR spectrum for rhodium-containing **13** shows a

Scheme 6. Synthetic Outline for Neutral Complexes **13** and **14**^a


^a All reactions were performed at 25 °C. All counterions are BF₄⁻.

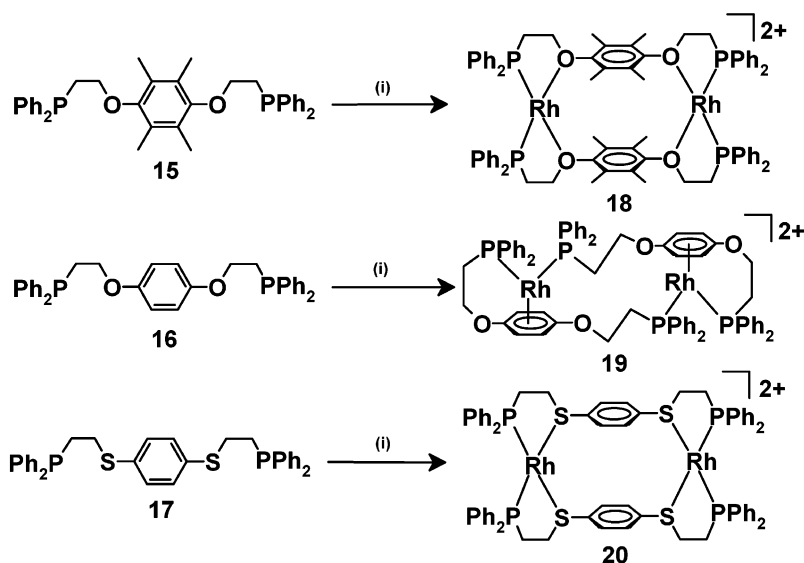
doublet at 21.3 ppm with $J_{\text{Rh-P}} = 122$ Hz, which is comparable to its benzene-based analogue (31 ppm, $J_{\text{Rh-P}} = 120$ Hz).^{3d} The ³¹P{¹H} NMR spectrum of iridium-containing **14** shows a singlet at 19.8 ppm, which is comparable to a mono-CO/Cl⁻ bis(phosphine) Ir^I bimetallic macrocycle.^{3g} The FT-IR spectra of **13** and **14** in CH₃NO₂ exhibit two broad ν_{CO} bands (1971, 2005 cm⁻¹ and 1973, 2015 cm⁻¹, respectively), which compare well with a Rh^I benzene-based analogue (1978, 2015 cm⁻¹)^{3g} and a mono-nuclear Ir^I bis CO/I⁻ bis(triphenylphosphine) complex (1935, 1995 cm⁻¹).¹⁴ The FT-IR spectroscopy data support the presence of 2 CO ligands/metal center in an equatorial arrangement.

Discussion and Conclusions

The rhodium(I) and iridium(I) metallomacrocycles reported herein demonstrate how one can control the chemistry about the metal centers of these complexes and their resulting properties via judicious choice of ligand substituents. The complexes previously generated via the weak-link approach provide a qualitative basis for the comparison of metal–weak link interaction strengths. Arene electron density

(13) Bryan, S. J.; Huggett, P. G.; Wade, K. *Coord. Chem. Rev.* **1982**, *44*, 149.

(14) Collman, J. P.; Vastine, F. D.; Roper, W. R. *J. Am. Chem. Soc.* **1968**, *90*, 2282.

Scheme 7. Synthetic Outline for Condensed Intermediates^a

^a All reactions were performed at $-78\text{ }^{\circ}\text{C}$. All counterions are BF_4^- . Reagents: (i) $[\text{Rh}(\text{COE})_2][\text{BF}_4]$, THF, CH_2Cl_2 .^{3b,d}

arguments (along with van der Waals interactions) have been used to explain the difference in the observed product distribution of reactions between metal precursors and similar bis(phosphinoalkyl ether)arene ligands **15** and **16** (Scheme 7).^{3a} This previous study suggests that the greater electron density of the arene core (due to the electron-donating methyl groups) in **15** increases the basicity of the ether moiety relative to **16**, which allows for a stronger Rh^{I} –ether bond to be formed. The electron density, in conjunction with increased van der Waals forces, allows for the exclusive formation of the *cis*-phosphine, *cis*-ether complex **18** from rhodium(I) metal center and ligand **15** while the analogous reaction with **16** gives the bis(phosphine) η^6 -arene complex **19** (Scheme 7).^{3b}

Other reports have shown that the metal–thioether bonds in condensed intermediates (e.g. **20**) are significantly stronger than their metal–ether analogues (e.g. **18**, Scheme 7).^{3d,3g} Indeed, the metal–thioether bonds of **20** are substitutionally inert under conditions that result in the displacement of the ether moieties in complex **18** (e.g., CO, MeCN, or both). To cleave the stronger metal–thioether interactions, either a halide-induced^{3d,g} or cyanide-induced^{3e} ring-opening approach is necessary (Scheme 1). Such approaches allow for the synthesis of neutral macrocyclic structures with tailorable cavity sizes and shapes. The synthesis of compounds **13** and **14** demonstrate that this pathway is also accessible to the fluorinated ligand systems reported herein.

The increased lability of the metal–thioether interactions in the complexes **2** and **3**, formed from ligand **1**, also allows one to use small molecule ligand substitution chemistry at the metal–thioether sites without the aid of anionic ligands,

such as halides or cyanide, to form the open macrocycles. This allows one to synthesize cationic macrocycles, such as **4–8**, which are analogous to cationic ether-containing macrocycles generated from complexes **18** and **19**. Thus far, cationic versions of thioether-containing macrocycles have not been accessible with ligands bearing substituents other than fluorine on the aromatic core. It is interesting to note that the fluorinated core substantially weakens the metal–thioether interactions yet yields thioether bonding moieties that are strong enough to guide the formation of the condensed intermediates (**2** and **3**) that are critical to the weak-link approach. The generation of these cationic structures with substitutionally labile metal centers allows for the sequestration of bifunctional organic molecules inside the cavity of the open macrocycles (Scheme 5). Taken together, these observations demonstrate how one can use aromatic substituents to adjust the bond strength between the metal center and the thioether moiety to yield a set of macrocycles with tailorable charge, reactivity, and pocket hydrophobicity.

Acknowledgment. C.A.M. acknowledges the NSF and AFOSR for support of this research.

Supporting Information Available: An ORTEP drawing of the X-ray structure of **2**, detailed X-ray structural data including a summary of crystallographic parameters, atomic coordinates, bond distances and angles, anisotropic thermal parameters, and H atom coordinates for **2** and **3**, and X-ray crystallographic files in CIF format. This material is available free of charge via the Internet at <http://pubs.acs.org>.

IC034393P